Spectroscopic Properties of Curcumin: Orientation of Transition Moments

ARTICLE *in* THE JOURNAL OF PHYSICAL CHEMISTRY B · OCTOBER 2010

Impact Factor: 3.3 · DOI: 10.1021/jp104075f · Source: PubMed

Enhanced Fluorescence of Curcumin on Plasmonic Platforms

Anindita Mukerjee[1], Rafal Luchowski[2,3,*], Amalendu P. Ranjan[1], Sangram Raut[2], Jamboor K. Vishwanatha[1], Zygmunt Gryczynski[2,4] and Ignacy Gryczynski[4,2,*]

[1]*Dept. of Molecular Biology & Immunology and Institute of the Cancer Research, UNTHSC, Fort Worth, TX 76107, USA;* [2]*Center for Commercialization of Fluorescence Technologies (CCFT), Dept. of Molecular Biology & Immunology, UNTHSC, Fort Worth, TX 76107, USA;* [3]*Dept. of Biophysics, Institute of Physics, Maria Curie-Sklodowska University, 20-031 Lublin, Poland;* [4]*Dept. of Cell Biology and Anatomy, UNTHSC, Fort Worth, TX 76107, USA*

Abstract: We report a significant increase of a curcumin (1,7-bis[4-hydroxy-3-methoxyphenyl]-1,6-heptadiene-3,5-dione) fluorescence brightness when deposited on plasmonic platforms (self assembled silver nanostructures formed on the surface of silver semitransparent film). The enhancement of fluorescence intensity is accompanied by a strong decrease in fluorescence lifetime. Simultaneously, the increased photostability of curcumin, a pigment showing strong anti-inflammatory, antioxidant and antitumorigenic activity, allows long-time detection and monitoring. We believe that the use of plasmonic platforms will improve detection, delivery and imaging of curcumin.

Keywords: Fluorescence lifetime, metal enhanced fluorescence, photostability, plasmonic platforms, brightness, curcumin.

1. INTRODUCTION

1.1. Metal Enhanced Fluorescence

The interest in a metal modified fluorescence originates with the discovery of Surface Enhanced Raman Scattering (SERS) [1-3]. In initial reports on fluorescence near rough silver surfaces, rather strong changes in lifetimes were accompanied with modest increases in brightness [4, 5]. This was slightly disappointing for the fluorescence community because during that same time gigantic enhancements in SERS were reported [6-8]. A significant limitation in case of fluorescence is a strong quenching at close proximity to the metal surface (below approximately 40-50 Angstroms). The fluorescence increase due to an enhanced local field near silver nanoparticles is therefore limited. The excited fluorophore, which acts as an oscillating dipole, may interact with localized plasmons in the metallic particle. This results in a deactivation of the excited molecule and rapid radiation of the excitation energy. The effect is known as radiative decay engineering (RDE) [9-11] which can be explained with an increase of radiative rate, which results in higher quantum yield and a shorter lifetime. Both, RDE and enhanced local field enhance the observed fluorescence. The total effect includes quenching and enhancement and is strongly dependent on the fluorophore-metal distance [12, 13]. Surface morphology also plays an important role. Stronger enhancements were observed on silver nanostructures with sharp edges like electrochemically deposited fractals [14, 15], weaker on smooth silver monolayers (suitable on the other hand for imaging) [16, 17]. Recently, we observed more than a 50-fold enhancement on silver island films deposited on gold or silver mirrors [18, 19], and more than 100-fold on self-assembled silver nanoparticles on metallic films [20, 21]. Such high enhancements are the result of localized (nanoparticle) and traveling (surface) plasmon interaction, which creates extremely strong local field. We call these substrates plasmonic platforms.

In this report we studied the fluorescence enhancement of curcumin-doped poly(vinyl alcohol) thin layer deposited either on bare glass cover slip or plasmonic platform.

1.2. Curcumin- a Natural Polyphenol Pigment

Over the past few decades, much research has been done to establish the pharmacological properties of curcumin, a yellow polyphenol, as well as the most active component extracted from the dried rhizome of the turmeric plant (*Curcuma longa*) belonging to the *zingiberaceae* family (Curcumin amount accounts for 2-8% of turmeric). Curcumin and some of its analogues are responsible for the bright yellow color of turmeric [22]. Curcumin's IUPAC name is (1E, 6E)–1,7-bis(4-hydroxy-3-methoxy phenyl)-1,6-heptadiene-3,5-dione. The chemical structure of curcumin (Fig. (**1**)) has two ortho-methoxy phenols attached symmetrically through α,β-unsaturated β-diketone linker, which also induces keto–enol tautomerism and imparts several interesting photophysical and photochemical properties to the curcumin molecule both in its solid state and solution. Among its pharmacological properties, it has been found that curcumin is a potent anti-inflammatory agent with strong therapeutic potential against a variety of cancers as it suppresses transformation, proliferation and metastasis of tumors. These effects are mediated through its regulation of various transcription factors like NF-κB, AP-1, growth factors, inflammatory cytokines, protein kinases like EGFR, HER2/neu and other enzymes [23]. Extensive research has been done to charac-

*Address correspondence to these authors at the Center for Commercialization of Fluorescence Technologies (CCFT), Dept. of Molecular Biology & Immunology, UNTHSC, Fort Worth, TX 76107, USA; Dept. of Biophysics, Institute of Physics, Maria Curie-Sklodowska University, 20-031 Lublin, Poland and Dept. of Cell Biology and Anatomy, UNTHSC, Fort Worth, TX 76107, USA; Tel: 8177352118; Fax: 8177352163;
E-mails: rluchows@hsc.unt.edu; igryczyn@hsc.unt.edu

1389-2010/10 $55.00+.00

terize this molecule for its physico-chemical and spectroscopic properties [24-27] as changes in the absorption and fluorescence properties of curcumin have been found useful in following its interaction and site of binding. Curcumin fluorescence could be employed to follow the unfolding pattern and structural changes in proteins. The intracellular curcumin showed greater fluorescence in tumor cells than in normal cells, and fluorescence spectroscopy could be used to monitor its preferential localization in the membranes of tumor cells [26].

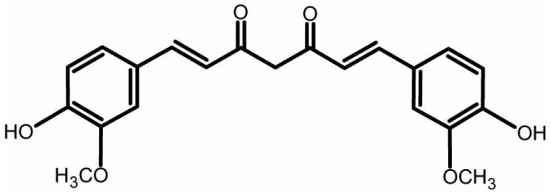

Fig. (1). Chemical structure of curcumin.

Among spectroscopic characterizations reported, the absorption maximum of curcumin is ~408-430nm in most of the organic solvents, while the emission maximum is very sensitive to the surrounding solvent medium (460-560 nm) and the Stokes' shift varied from 2000 to 6000 cm^{-1}. The fluorescence quantum yield in most of the solvents is low and reduced significantly in the presence of water. The fluorescence lifetime was short (<1 ns) and displayed a multi-exponential decay profile.

Because of its profound effect on human health, the detection, dosage control and imaging of curcumin are of great interest to medical and pharmaceutical researchers. However, in many fluorescence studies photostability as well as poor quantum efficiency and weak brightness are bottlenecks. In this manuscript, we demonstrate that curcumin fluorescence intensity and its photostability can be significantly enhanced in the presence of silver nanostructures.

2. MATERIALS AND METHODS

2.1. Preparation of Plasmonic Platforms

Plasmonic platform consists of silver nanostructures located on the surface of a noble metal; in our case these are self-assembled colloidal structures (SACS) evaporated on a silver semitransparent mirror. These mirrors (microscope cover slips coated with 54nm thick silver layer and protected with 10nm SiO2) were prepared by EMF, Inc., Ithaca, NY.

The silver colloids were made as previously described [28]. Briefly, all necessary glassware was soaked in a base bath overnight and washed scrupulously with deionized water. The solution of 0.18 mg/mL silver nitrate (200 mL) was heated and stirred in a 250 mL Erlenmeyer flask at 95°C. The first 0.5 mL aliquot of 34 mM trisodium citrate solution was added dropwise. The solution was stirred for 20 min and warmed to 96-98°C. Then five aliquots (0.7 mL each) of 34 mM trisodium citrate were added dropwise to the reaction mixture every 15-20 min. Stirring was continued for 25 min until the milky yellow color was achieved. Then the mixture was cooled in an ice bath for 15 min. Silver colloids were then used to prepare SACS. Slide surfaces were cleaned and drop coated with silver colloids. The slides were air dried to form SACS. The dry slides with self-assembled nanoparticles were stored and used within a month.

2.2. Atomic Force Microscopy (AFM) Measurements

AFM images were taken on an Explorer Scanning Probe Microscope. Samples were imaged with showing a 25x25 micrometer area at a 300x300 pixel resolution in a contact mode. All images were processed and analyzed with a Veeco DI SPMLab software.

2.3. Curcumin-PVA Thin Layer Deposition

Curcumin (97% pure) was obtained from the Sabinsa Corporation, NJ, USA, and used without further purification. Poly (Vinyl Alcohol), MW 10,000 was from Aldrich, Inc.

The solution of curcumin in 0.25% of low molecular weight PVA was used for covering sample slides with a thin layer of curcumin-doped polymer. The deposition was done using a spin-coater (Specialty coating systems, Inc. IN 46278) model P6700 at 3,000 rpm for 120s.

2.4. Spectroscopic Measurements

Fluorescence spectroscopic measurements were done in front-face mode using FluoTime 200 fluorometer (PicoQuant, GmbH, Berlin, Germany). This time-resolved instrument is equipped with an ultrafast detector, a Hamamatsu R3809U-50 microchannel plate photomultiplier (MCP). For the excitation we used a 405nm picosecond pulsed laser diode. The detection was from a monochromator supported with two 450nm long wave pass filters in order to eliminate a scattering excitation light. The decay data were analyzed with FluoFit, version 5.0 software (PicoQuant, GmbH). Fluorescence intensity decays were analyzed by reconvolution with the instrument response function and analyzed as a sum of exponential terms:

$$I(t) = \sum_i \alpha_i \exp(-t/\tau_i) \quad (1)$$

where I(t) is the fluorescence intensity at time t and α_i is a pre-exponential factor representing the fractional contribution to the time-resolved decay of the component with a lifetime τ_i ($\sum\alpha_i = 1$). The amplitude average lifetime was calculated as $\langle\tau\rangle = \sum_i \alpha_i \tau_i$.

2.5. Time-Resolved Fluorescence Microscopy

Simultaneous fluorescence intensity and lifetime measurements were taken at the same experimental conditions on a MicroTime 200 (PicoQuant, GmbH) confocal fluorescence microscopy system with lifetime imaging. The excitation was done by a 405nm laser pulsed diode modulated at 40 MHz and focused on the sample using a high numerical aperture (NA) objective (Olympus 60x magnification, NA 1.2, water immersed). Observation was through a system of three 450nm long wave pass filters and the fluorescence signal was detected by a Perkin-Elmer SPCM-AQR-14 detector in the mode of a time correlated single photon counting. Decay data were analyzed with the SymPhoTime (version 5.0) software package that controlled the data acquisition as well.

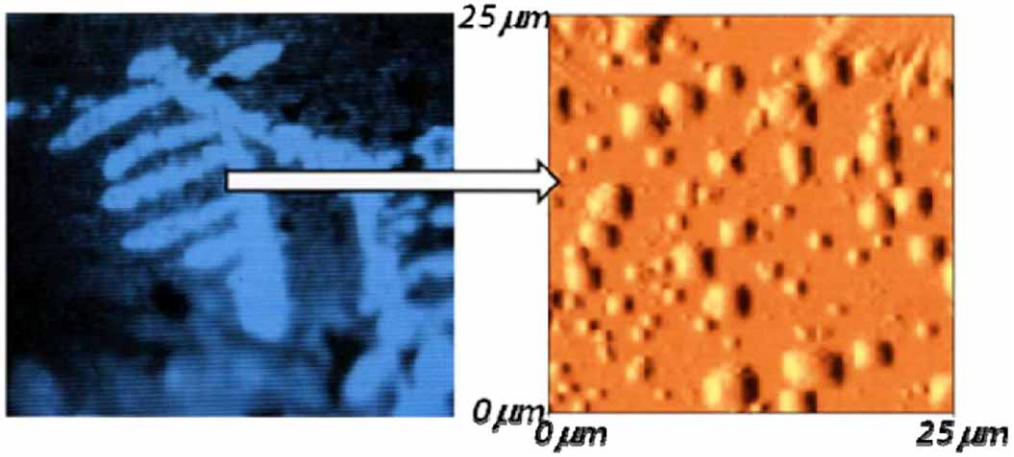

Fig. (2). Morphology photograph taken from AFM monitor (left) and AFM image of plasmonic platform (right).

3. RESULTS

The self-assembled colloidal structures (SACS) prepared on the silver semitransparent mirror were evaluated with AFM (Fig. (**2**)). Upon evaporation, the colloids form prism-like groups of silver nanoparticles. Near these groups, the local electromagnetic field (as an effect of localized and traveling plasmons interaction) is strongly enhanced, and therefore fluorophores deposited on them will be excited more efficiently. Also, excited fluorophores will interact with silver nanostructures inducing plasmons due to the excitation energy (RDE effect). We expect an enhanced brightness and a shorter lifetime from curcumin deposited on the plasmonic platform compared to bare glass.

Fig. (**3**) shows fluorescence emission spectra of a curcumin doped PVA thin layer on glass and plasmonic platform. As expected, fluorescence emission is more than 10-fold stronger on the plasmonic platform than on glass.

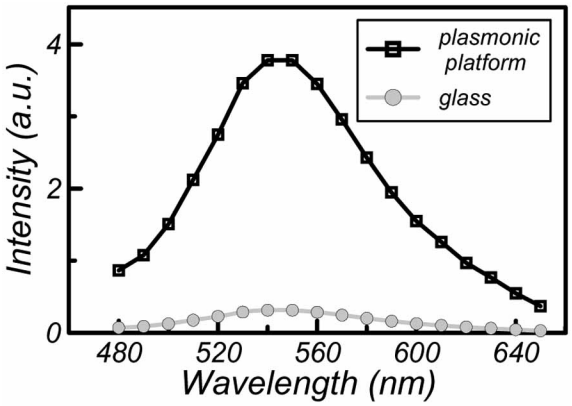

Fig. (3). Fluorescence spectra of curcumin-doped PVA thin layer deposited on glass and plasmonic platform.

Next, we measured the intensity decays of curcumin doped PVA on glass (Fig. (**4**)) and on the plasmonic platform (Fig. (**5**)). On the glass, the decay is almost single exponential with an amplitude averaged lifetime of about 1ns. In contrast, on the plasmonic platform the decay is strongly heterogeneous with an average lifetime of about 30ps. Such a strong decrease in lifetime in combination with the increased brightness indicates an efficient RDE effect.

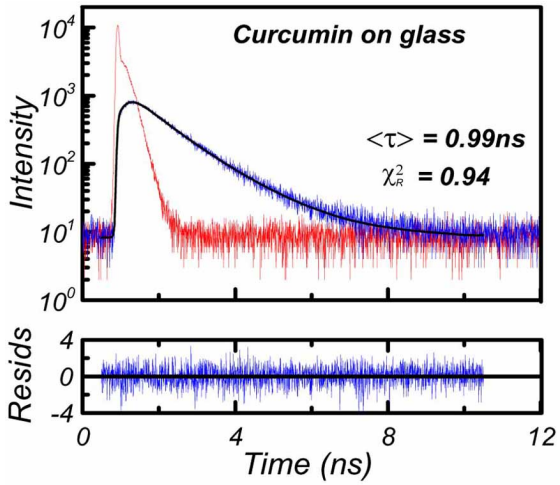

Fig. (4). Fluorescence intensity decay of curcumin-doped PVA thin layer deposited on glass. The decay is almost homogeneous with the lifetime of about 1ns.

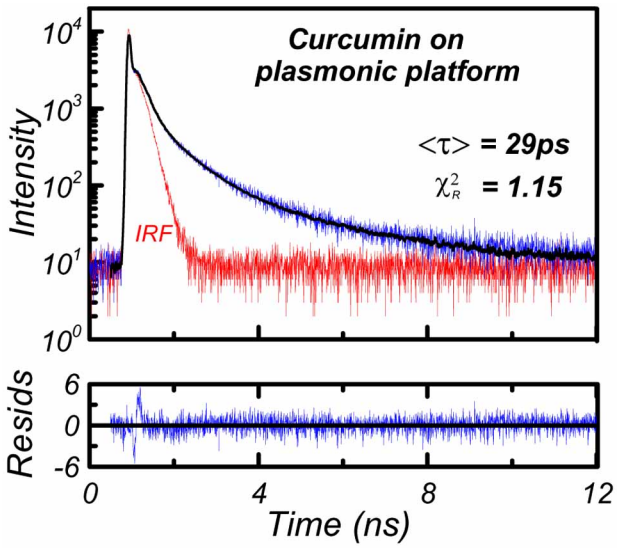

Fig. (5). Fluorescence intensity decay of curcumin-doped PVA thin layer deposited on plasmonic platform. The decay is highly heterogeneous with amplitude averaged lifetime of 29ps.

It should be noted that the illumination spot was about 1mm^2 large and the total emission is an averaged value. We expect that the morphologies of samples deposited on glass and plasmonic platforms are different.

Therefore we investigated both samples with a time-resolved confocal microscope.

The confocal images are presented in Fig. (**6**). Both brightness and lifetimes are distributed homogeneously for the sample deposited on the glass cover slip (Fig. (**6**), right). In the case of plasmonic platform (Fig. (**6**), left), the brightness and lifetimes are distributed non-uniformly, indicating "hot spots" with brightness hundred times stronger than in other places. Interestingly, stronger brightness corresponds to shorter lifetime, and where brightness is weaker, the lifetime is longer.

Finally, we measured how quickly samples photodegrade (Fig. **7**). The excitation power was adjusted to yield the same fluorescence intensity at the beginning of the experiment. Within two minutes the sample on glass lost about 80% of brightness. The sample on the plasmonic platform in the same time lost only a few percent of its brightness.

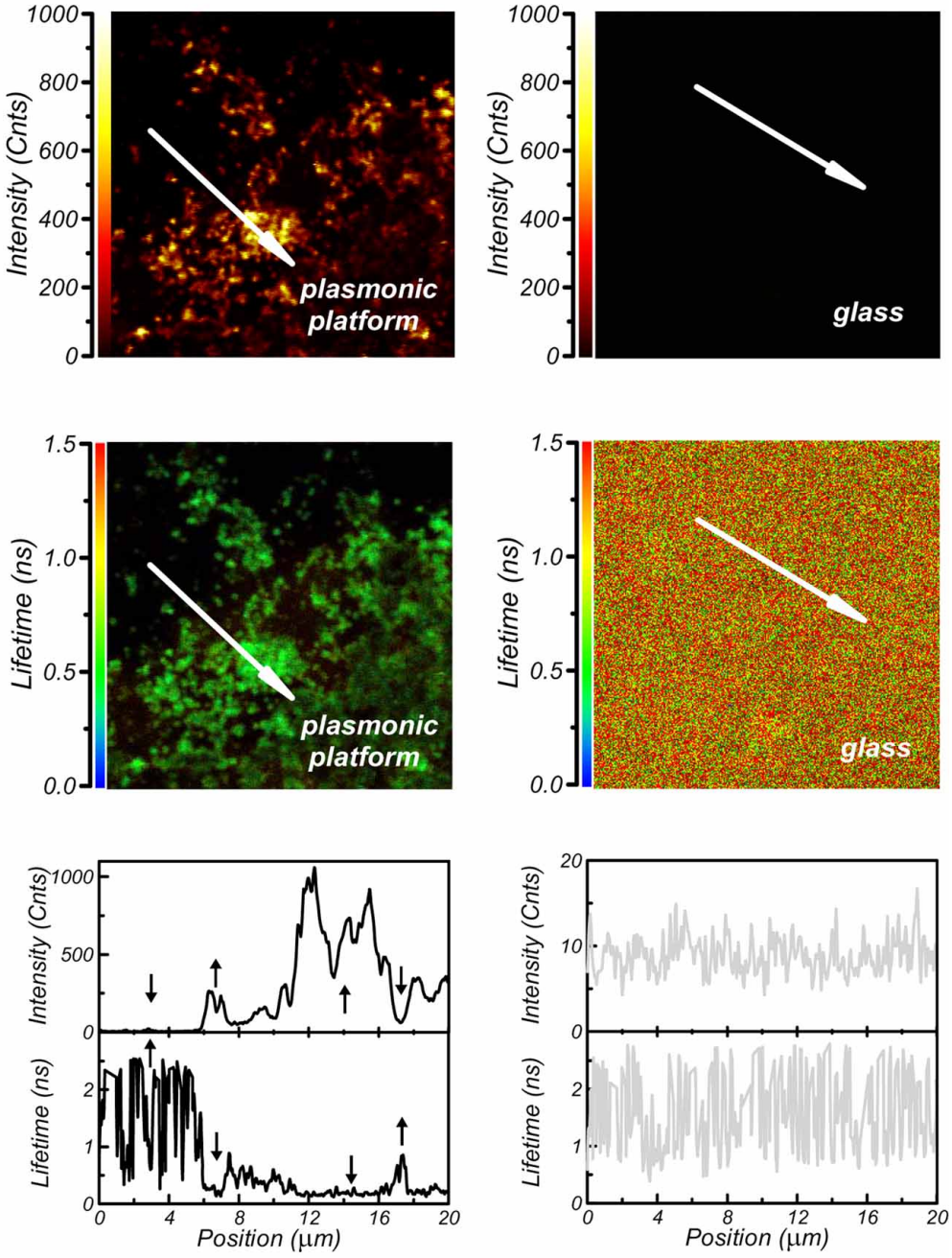

Fig. (6). Intensity and lifetime microscopy images of curcumin deposited on glass (top, right) and plasmonic platform (top, left). Intensity and lifetime distributions taken along lines indicated on images for curcumin deposited on glass (bottom, right) and plasmonic platform (bottom, left). The strongest fluorescence intensities and shortest lifetimes are observed on/near self assembled silver nanostructures.

4. CONCLUSIONS

Why is curcumin fluorescence so strongly enhanced on plasmonic platforms? There are two effects responsible for this. First, the excitation field is strongly amplified around silver nanostructures deposited on a conductive surface. Locally, in "hot spots" the effect is very significant (see Fig. (**6**)). The second effect, RDE, is also relatively strong in the case of curcumin. The quantum efficiency of curcumin is low; therefore the possible gain in quantum yield is higher than for highly bright dyes. The change in a radiative rate of curcumin on the plasmonic platform is significant, with the rough estimation about 50 fold (the ratio of lifetimes on glass and plasmonic platform). In addition, the photostability of curcumin on the plasmonic platform is much better than on glass substrates. All described above effects indicate that the detection range of curcumin can be lowered on plasmonic platforms by two to three orders of magnitude. We also believe that with the proposed technology the monitoring and imaging of curcumin will be improved as well.

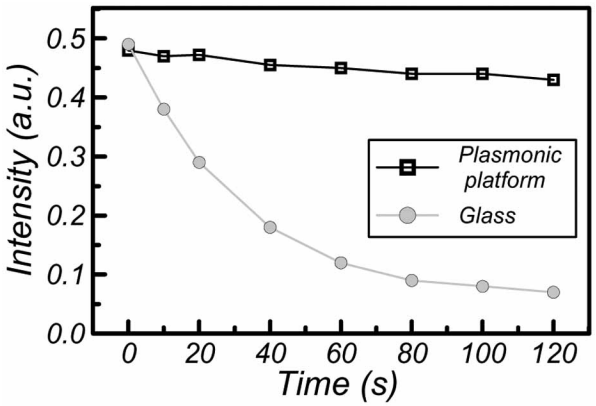

Fig. (7). Photobleaching of curcumin deposited on glass and plasmonic platform. Reduced lifetime resulted in increased photostability.

ACKNOWLEDGEMENTS

This work was supported by Texas ETF (CCFT), DOD grant W81XWH-09-1-0406 (Z.G.), and RP0009 from SignPath Pharmaceuticals Inc, PA, USA (JKV). We thank Dr. Lawrence Helson (SignPath Pharmaceuticals Inc., PA, USA) for curcumin; Dr. Tanya Shtoyko for silver colloids preparation and Dr. Irina Akopova for AFM images.

REFERENCES

[1] Fleischmann, M.; Hendra, P. J.; McQuillan, A. J. Raman spectra of pyridine at a silver electrode. *Chem. Phys. Lett.*, **1974**, *26*, 163-166.

[2] Jeanmaire, D. L.; Van Duyne, R. P. Surface Raman spectroelectrochemistry. Part I. Heterocyclic, aromatic, and aliphatic amines adsorbed on the anodized silver electrode. *J. Electroanal. Chem.*, **1977**, *84*, 1-20.

[3] Philpott, M. R. Effect of surface plasmons on transition in molecules. *J. Chem. Phys.*, **1975**, *62*, 1812-1817.

[4] Aussenegg, F. R.; Leitner, A.; Lippitsch, M. E.; Reinisch, H.; Riegler, M. Novel aspects of fluorescence lifetime for molecules positioned close to metal surfaces. *Surf. Sci.*, **1987**, *189-190*, 935-945.

[5] Leitner, A.; Lippitsch, M. E.; Draxler, S.; Riegler, M.; Aussenegg, F. R. Fluorescence properties of dyes adsorbed to silver islands, investigated by picosecond techniques. *Appl. Phys. B*, **1985**, *36*, 105-109.

[6] Camden, J. P.; Dieringer, J. A.; Wang, Y. M.; Masiello, D. J.; Marks, L. D.; Schatz, G. C.; Van Duyne, R. P. Probing the structure of single-molecule surface-enhanced Raman scattering hot spots. *J. Am. Chem. Soc.*, **2008**, *130*(38), 12616-12617.

[7] Kneipp, K.; Kneipp, H.; Itzkan, I.; Dasari, R. R.; Feld, M. S. Surface-enhanced Raman scattering: A new tool for biomedical spectroscopy. *Curr. Sci.*, **1999**, *77*(7), 915-924.

[8] McMahon, J. M.; Henry, A.-I.; Wustholz, K. L.; Natan, M. J.; Freeman, G.; Van Duyne, R. P.; Schatz, G. C. Gold nanoparticle dimer plasmonics: finite element method calculations of the electromagnetic enhancement to surface-enhanced Raman spectroscopy. *Anal. Bioanal. Chem.*, **2009**, *394*, 1819-1825.

[9] Lakowicz, J.R. Radiative decay engineering: biophysica and biomedical applications. *Anal. Biochem.*, **2001**, *298*, 1-24.

[10] Lakowicz, J.R. *Radiative decay engineering: metal enhanced fluorescence*, 3rd ed.; Springer: New York, **2003**, pp. 841-859.

[11] Lakowicz, J. R.; Shen, Y.; D'Auria, S.; Malicka, J.; Fang, J.; Gryczynski, Z.; Gryczynski, I. Radiative decay engineering. 2. Effects of Silver Island films on fluorescence intensity, lifetimes, and resonance energy transfer. *Anal. Biochem.*, **2002**, *301*(2), 261-277.

[12] Malicka, J.; Gryczynski, I.; Gryczynski, Z.; Lakowicz, J. R. Effects of fluorophore-to-silver distance on the emission of cyanine-dye-labeled oligonucleotides. *Anal. Biochem.*, **2003**, *315*(1), 57-66.

[13] Sokolov, K.; Chumanov, G.; Cotton, T. M. Enhancement of molecular fluorescence near the surface of colloidal metal films. *Anal. Chem.*, **1998**, *70*(18), 3898-3905.

[14] Parfenov, A.; Gryczynski, I.; Malicka, J.; Geddes, C. D.; Lakowicz, J. R. Enhanced fluorescence from fluorophores on fractal silver surfaces. *J. Phys. Chem. B*, **2003**, *107*(34), 8829-8833.

[15] Shtoyko, T.; Matveeva, E. G.; Chang, I. F.; Gryczynski, Z.; Goldys, E.; Gryczynski, I. Enhanced fluorescent immunoassays on silver fractal-like structures. *Anal. Chem.*, **2008**, *80*(6), 1962-1966.

[16] Borejdo, J.; Muthu, P.; Talent, J.; Gryczynski, Z.; Calander, N.; Akopova, I.; Shtoyko, T.; Gryczynski, I. Reduction of photobleaching and photodamage in single molecule detection: observing single actin monomer in skeletal myofibrils. *J. Biomed. Opt.*, **2008**, *13*(3): 034021.

[17] Muthu, P.; Calander, N.; Gryczynski, I.; Gryczynski, Z.; Talent, J. M.; Shtoyko, T.; Akopova, I.; Borejdo, J. Monolayers of silver nanoparticles decrease photobleaching: Application to muscle myofibrils. *Biophys. J.*, **2008**, *95*(7), 3429-3438.

[18] Barnett, A.; Matveeva, E. G.; Gryczynski, I.; Gryczynski, Z.; Goldys, E. M. Coupled plasmon effects for the enhancement of fluorescent immunoassays. *Phys. B*, **2007**, *394*, 297-300.

[19] Matveeva, E. G.; Gryczynski, I.; Barnett, A.; Leonenko, Z.; Lakowicz, J. R.; Gryczynski, Z. Metal particle-enhanced fluorescent immunoassays on metal mirrors. *Anal. Biochem.*, **2007**, *363*(2), 239-245.

[20] Luchowski, R.; Matveeva, E. G.; Shtoyko, T.; Sarkar, P.; Patsenker, L. D.; Klochko, O. P.; Terpetschnig, E. A.; Borejdo, J.; Akopova, I.; Gryczynski, Z.; Gryczynski, I. Single molecule immunoassay on plasmonic platforms. *Curr. Pharm. Biotechnol.*, **2010**, *11*(1), 96-102.

[21] Sorensen, T. J.; Laursen, B. W.; Luchowski, R.; Shtoyko, T.; Akopova, I.; Gryczynski, Z.; Gryczynski, I. Enhanced fluorescence emission of Me-ADOTA(+) by self-assembled silver nanoparticles on a gold film. *Chem. Phys. Lett.*, **2009**, *476*(1-3), 46-50.

[22] Adhikary, R.; Mukherjee, P.; Kee, T. W.; Petrich, J. W. Excited-state intramolecular hydrogen atom transfer and solvation dynamics of the medicinal pigment curcumin. *J. Phys. Chem. B*, **2009**, *113*(15), 5255-5261.

[23] Shishodia, S.; Chaturvedi, M. M.; Aggarwal, B. B. Role of curcumin in cancer therapy. *Curr. Probl. Cancer*, **2007**, *31*(4), 243-305.

[24] Barik, A.; Priyadarsini, K. I.; Mohan, H. Photophysical studies on binding of curcumin to bovine serum albumin. *Photochem. Photobiol.*, **2003**, *77*(6), 597-603.

[25] Khopde, S. M.; Priyadarsini, K.; Palit, D. K.; Mukherjee, T. Effect of solvent on the excited-state photophysical properties of curcumin. *Photochem. Photobiol.*, **2000**, *72*(5), 625-631.

[26] Priyadarsini, K. I. Photophysics, photochemistry and photobiology of curcumin: Studies from organic solutions, bio-mimetics and living cells. *J. Photochem. Photobiol. C-Photochem. Rev.*, **2009**, *10*(2), 81-95.

[27] Scotter, M. J. Synthesis and chemical characterisation of curcuminoid colouring principles for their potential use as HPLC standards

for the determination of curcumin colour in foods. *Lwt-Food Sci. Technol.*, **2009**, *42*(8), 1345-1351.

[28] Lukomska, J.; Gryczynski, I.; Malicka, J.; Makowiec, S.; Lakowicz, J. R.; Gryczynski, Z. One- and two-photon induced fluorescence of pacific blue-labeled human serum albumin deposited on different core size silver colloids. *Biopolymers*, **2006**, *81*(4), 249-255.

Received: January 21, 2010 **Accepted: January 22, 2010**